INTERNATIONAL SOCIETY FOR SOIL MECHANICS AND GEOTECHNICAL ENGINEERING



This paper was downloaded from the Online Library of the International Society for Soil Mechanics and Geotechnical Engineering (ISSMGE). The library is available here:

https://www.issmge.org/publications/online-library

This is an open-access database that archives thousands of papers published under the Auspices of the ISSMGE and maintained by the Innovation and Development Committee of ISSMGE.

A coupled CFD-DEM study of debris flow impacts: the influence of mass exchange

Xingyue LI, Jidong ZHAO

Department of Civil and Environmental Engineering, Hong Kong University of Science and Technology, Hong Kong, xlibp@ust.hk

ABSTRACT: Key to the design of effective mitigation measures for debris flow lies in accurate assessments of its kinematics and impacts. A coupled Computational Fluid Dynamics and Discrete Element Method (CFD-DEM) approach is employed in this study to model debris flow as a mixture of fluid and solid phases. In so doing, the mixing process of the two phases during the flow of a debris and their separate impacts can be differentiated and evaluated reliably. Frequently, the solid phase in debris flow may contain loosely-packed aggregates coming from either the sources sites or entrainment which may break into fines and greatly affect the kinematic behaviour for both solid and fluid phase. We consider the breakage of aggregates into fines by exchanging mass between the solid phase and fluid phase and henceforth corresponding change of properties for the two phases in our simulation. The influence of fine contents added into the fluid phase from the solid phase is carefully examined. It is found that the mobility and impacts of debris flow are enhanced by increased fine contents added to the fluid phase, and the flow patterns and kinematics can be greatly changed as well. Correlation of the obtained empirical coefficient of impact model based on the numerical study agrees well with experimental data.

RÉSUMÉ: La conception de mesures efficaces d'atténuation du flux de débris est essentielle à l'évaluation précise de sa cinématique et de ses impacts. Une approche de la dynamique des fluides computationnelle couplée et de l'élément discret (CFD-DEM) est utilisée dans cette étude pour modéliser le flux de débris sous forme de mélange de phases fluide et solide. Ce faisant, on peut différencier et évaluer de manière fiable le processus de mélange des deux phases pendant le flux des débris et leurs impacts séparés. Souvent, la phase solide dans l'écoulement des débris peut contenir des agrégats lâches emballés provenant des sites sources ou de l'entraînement qui peuvent se rompre en fines et affecter fortement le comportement cinématique à la fois pour la phase solide et la phase fluide. Nous considérons la rupture des agrégats en fines par échange de masse entre la phase solide et la phase fluide et donc le changement de propriétés correspondant pour les deux phases dans notre simulation. L'influence du contenu fin ajouté dans la phase fluide de la phase solide est soigneusement examinée. On constate que la mobilité et les impacts du flux de débris sont améliorés par l'augmentation du contenu fin ajouté à la phase fluide, et les schémas d'écoulement et la cinématique peuvent également être grandement modifiés. La corrélation du modèle de coefficient d'impact empirique obtenu basé sur l'étude numérique s'accorde bien avec les données expérimentales.

KEYWORDS: Coupled CFD-DEM, debris flow, mass exchange, impacting.

1 INTRODUCTION

To capture the non-linear behaviour of debris flow, non-Newtonian constitutive relations, such as Herschel-Bulkley model, have recently been adopted in various numerical simulations (Wang et al. 2016; Leonardi et al. 2013). The continuum-based approaches, however, have apparent pitfalls in capturing the complicated mixing processes during the flow of a debris and its impacts on an obstacle, especially when such processes as entrainment, deposition and breakage of solid particles occur in the course of flowing and impacting (Iverson 2003, Arabnia 2015). In particular, the fraction of fines in a debris may increase substantially in the flow from various sources such as entrainment and aggregate breaking, which may give rise to considerable changes of the density and the effective viscosity for the fluid (Iverson 1997). The overall dynamic responses will hereby be influenced (Ilstad et al. 2004). In this study, we consider the mass exchange between the solid and fluid phases in a debris mixture, and assess its effect on the overall kinematics of the debris flow and its impacting on an obstacle. We employ a coupled CFD-DEM approach, where the CFD is used to treat the fluid phase of a debris mixture comprised of water and fine particles and the DEM is applied to model the solid phase consisting of coarse particles (Zhao and Shan 2013a, Zhao and Shan 2013b, Shan and Zhao 2014). Mass exchange between the DEM and CFD simulations is detailed in the following.

2 METHODOLOGY

In the coupled CFD-DEM approach, the DEM (Cundall and Strack, 1979) is used to treat the particle system by solving Newton's equations governing the translational and rotational

motions of each particle in the system. The fluid system in the mixture is simulated by the CFD which solves the locally averaged Navier-Stokes equation for each fluid cell. The CFD and DEM exchange information on the fluid-particle interaction forces, including buoyancy force, drag force and viscous force (Kafui et al., 2002; O'Sullivan 2011; Zhou et al., 2010; Koch and Hill, 2001).

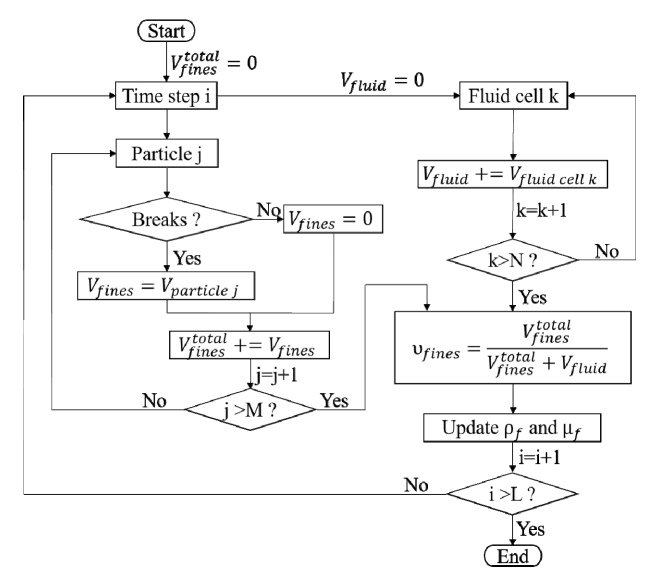


Figure 1. Flow chart on calculation of fraction of fines, fluid density and effective viscosity ($V_{\rm fines}^{\rm total}$ is the total volume of fines; $V_{\rm fluid}$ is the volume of original fluid; $V_{\rm fines}$ is the volume of fines; $V_{\rm fluid}$ cell k; $v_{\rm fines}$ is the fraction of fines; M is the total number of breakable particles representing clumps of fines; N is the total number of fluid cells with particles inside; L is the final time step).

T 11 1		1.1	1 . 10 .1	1 LOED DI	73.6
Table I	Summary of	model parameter	s adopted for the	counted CFD-DI	∃M simulation

Unbreakable particle	Diameter	0.02 m
	Density	2500
	Young's modulus	70 GPa
	Poisson's ratio	0.3
	Restitution coefficient	0.7
	Interparticle friction coefficient	0.7
	Rolling fraction coefficient	0.1
Breakable particle	Diameter	0.012m
-	Density	2000
	Young's modulus	70 MPa
	Poisson's ratio	0.3
	Restitution coefficient	0.3
	Interparticle friction coefficient	0.7
	Rolling fraction coefficient	0.1
Water	Density	1000kg/m^3
	Viscosity	0.001 Pa.s
Air	Density	1kg/ m^3
	Viscosity	1.48×10 ⁻⁵ Pa.s
Simulation control	Time step (CFD)	5×10 ⁻⁶ s
	Time step (DEM)	5×10 ⁻⁷ s
	Simulated real time	10 s

Fig. 1 shows the flow chart calculating the mass exchange between the solid and fluid phases. For a breakable particle j in the solid phase, we check its breakage according a prescribed breakage criterion. If particle j breaks into fines, it will be removed from the particle system and simultaneously its volume $V_{particle\ j}$ will be transformed into a volume of fines V_{fines}^{total} to be considered in the fluid. For the fluid system, the total fluid volume of a cell with particles inside V_{fluid} is calculated to obtain the fraction of fines defined as follows (Iverson 1997):

$$\upsilon_{\text{fires}} = V_{\text{fires}}^{\text{total}} / V_{\text{fluid phase}} = V_{\text{fires}}^{\text{total}} / (V_{\text{fires}}^{\text{total}} + V_{\text{fluid}})$$
 (1)

The density ρ_f and effective viscosity μ_f of the fluid are subsequently updated (Iverson 1997) only for fluid cells containing solid particles in order to mimic the dissolving of fines by the nearby fluid rather than the whole fluid phase:

$$\rho_f = \rho_s \nu_{\text{fines}} + \rho_{\text{tr}} (1 - \nu_{\text{fines}}) \tag{2}$$

$$\mu_r = \mu_{rr} (1 + 2.5 \nu_{\text{flux}} + 10.05 \nu_{\text{flux}}^2 + 0.00273 \exp(16.6 \nu_{\text{flux}}))$$
 (3)

where ρ_s and ρ_{pf} are respectively the densities of the particle and original fluid, and μ_{pf} and μ_f are the effective viscosity of the original fluid and the new fluid phase with added fines, respectively. The effective viscosity reflects not only the dynamic viscosity but also the yield stress of the fluid. It is calculated for a Herschel-Bulkley fluid as follows:

$$\mu_{r} = \tau / \dot{\gamma} = (\tau_{0} + \kappa \dot{\gamma}^{p}) / \dot{\gamma} \tag{4}$$

where τ is the fluid shear stress, τ_0 is the yield stress, κ is the consistency, $\dot{\gamma}$ is the shear strain rate and n is the flow index. If n=1, the fluid becomes a Bingham fluid and the consistency κ is indeed the fluid dynamic viscosity.

3 RESULTS AND DISCUSSION

3.1 Model setup

Fig. 2 shows the model setup for the simulation of debris flow impacting on a rigid barrier. A cubic mixture composed by particles and water is initially confined on top of an inclined channel with a slope angle of 35°, and is then released to collapse onto the slope channel and to impact on the rigid barrier. As summarized in Table 1, there are two types of

particles used for the cubic mixture, one breakable and the other not. While the initial fluid phase in the cubic mixture is water, as the breakable particles are broken into fines and dissolved into the fluid phase, the fluid changes from pure water to a viscous non-Newtonian fluid during the flowing process. The dimensions of model setup are shown in Fig. 1 and the parameters adopted in simulations are summarized in Table 1. With a fixed volume of the mixture (0.5m*0.4m*0.4m) and the solid phase (0.5m*0.4m*0.3m), this study investigates 8 cases with various fractions of fines as listed in Table 2.

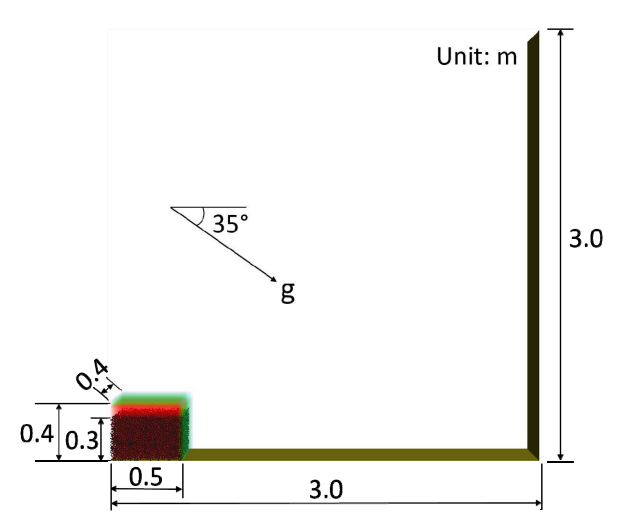


Figure 2. Model setup of a debris flow impacting on a rigid barrier.

Table 2. Summary of eight simulated cases for the study.

2. Summary of eight simulated cases for the study.								
	Case	Number of	Number of	Fraction of				
	ID	breakable	unbreakable	fines v_{fines}				
		particles	particles					
	1	0	8561	0				
	2	4967	7712	16.23%				
	3	9784	6780	28.01%				
	4	13950	5721	35.03%				
	5	18990	4933	43.68%				
	6	23230	4022	48.71%				
	7	25264	3585	50.82%				
	8	27346	3136	52.80%				

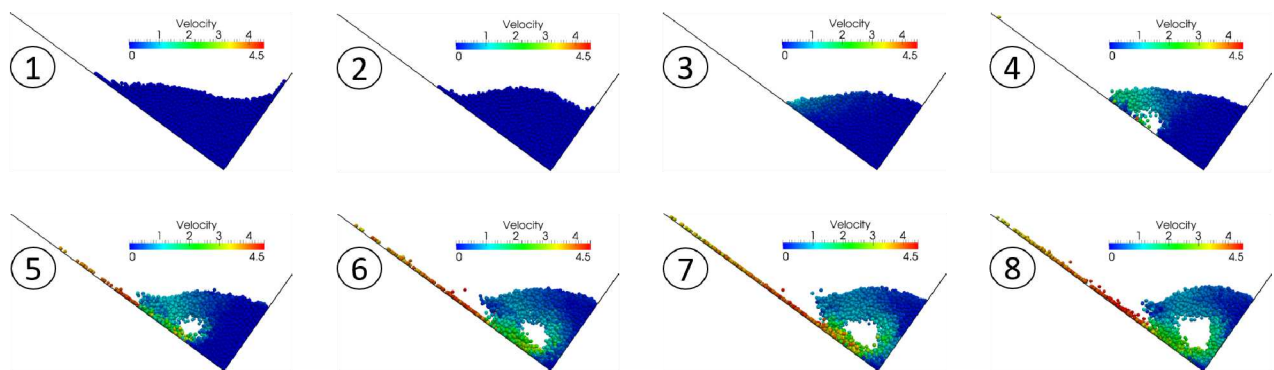


Figure 3. Profile of the granular system at t = 4.0 s for the eight cases in Table 2.

3.2 Profile evolution

Fig. 3 compares the debris profiles for difference cases with varying fraction of fines at a time instant t = 4 s wherein only the granular system is showed and the fluid phase has an overall similar contour with solid phase during the movement. In contrast to a nearly stable state observed in Cases 1~3, it is evident from Fig. 3 that in Cases 4~8 a vortex-like flow pattern is observed. Similar vortex-like flow pattern has indeed been discovered in experimental tests (Canelli et al. 2012). For Cases 1~3, the large portion of unbreakable particles in the solid phase effectively reduce the mobility of the debris mixture where no vortex-like flow patterns are found. The small fraction of fines added to the fluid phase has limited effects in enhancing the fluid phase to drag the solid phase. When the fraction of fines become larger in Cases 4~8, they add to increased fluid density and effective viscosity for the fluid phase and result in a dominant role of the fluid against the solid phase and high mobility of the entire mixture. The occurrence of vortex-like flow pattern observed in Cases 4~8 is mainly a result of the enhanced mobility, high kinetic energy and large turbulence intensity (see Hua and Jermy 2011).

3.3 Impact signal

A key step for debris barrier design is the assessment of impact load. The coupled CFD-DEM approached employed by this study offers us the convenience to separate the contributions of impact force from the solid and fluid phases and to examine the effect of fine exchange on the impacting. The impact force from the solid phase is calculated by summing up all contact forces between the rigid barrier and those contacted particles, whilst the impact force from the fluid is obtained by multiplying the barrier area by the fluid pressure on the barrier. The total impact force is an addition of these two. To reduce randomness in the results, the crude data on the impact force are averaged to attain a relatively smooth curve which retains the characteristic shape of the original one (Yang et al. 2011, Scheidl et al. 2013).

Fig. 4 (a) and (b) demonstrate two representative cases with a lower and higher fraction of fines. For both cases, the total impact force (in solid black line) increases sharply upon the collapse of the debris mixture onto the barrier and reaches a first local peak A shortly before a drop. The drop is induced by the decreased momentum change within the debris mixture along the direction orthogonal to the barrier, since the flow rate of mass flowing from the slope channel to the rigid barrier becomes smaller. Notably, this reduction in Case 6 is more severe than that in Case 2, indicating a higher mobility of the debris mixture in Case 6. In both case, the total impact force experiences a dramatic increase from around t = 2 s to peak B, due mainly to two reasons: (1) the significant increase in momentum change within the debris mixture and (2) the growing volume of the debris mixture continuously moving

from the slope channel toward the barrier. The maximum total impact force at peak B in Case 6 is markedly larger than that in Case 2 due to the higher kinetic energy and more fierce dynamic impact caused by the fluid added by higher fraction of fines. The post-peak decrease and the followed increase from B to C is induced by the repulsive wave from the barrier to the channel slope and subsequent moving back. In comparison with Case 2, the more fluctuated curve of total impact force near peak C in Case 6 is a result of the vortex-like flow pattern observed in Fig. 3. The increased fluctuations in Case 6 are indeed consistent with the wavy nature of the mixture dominated by the fluid phase, which is evident from an almost identical curve of the impact force contributed from the fluid (in short dash line) with the total impact force curve in Case 6 in contrast to a large difference in Case 2.

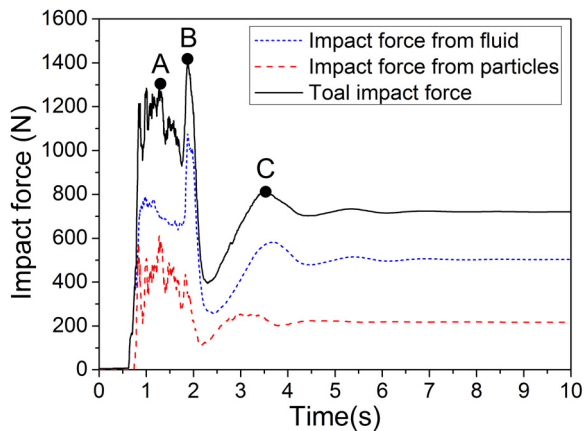


Figure 4a. Impact force contributed from the fluid phase, the solid phase and the overall debris mixture in Case 2 with v_{fines} = 16.23%.

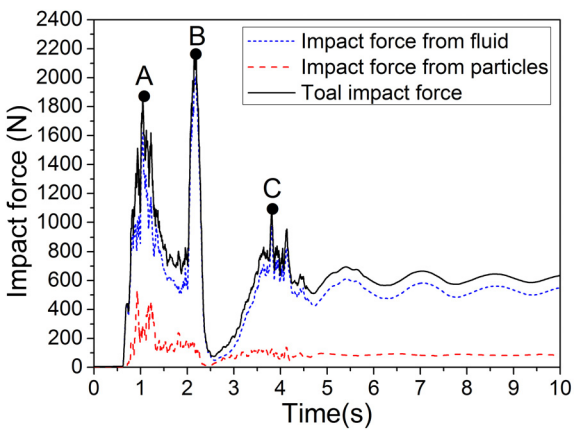


Figure 4b. Impact force contributed from the fluid phase, the solid phase and the overall debris mixture in Case 6 with v_{fines} = 48.71%.

3.4 Correlation between empirical coefficient and Froude number

An empirical hydrodynamic model widely used to estimate the impact pressure of debris flow reads as follows (Cui et al. 2015):

$$P = \alpha \rho_t v^2 \tag{5}$$

where P is the debris flow dynamic pressure, ρ_f and v are the debris flow density and velocity, respectively. The empirical coefficient α is correlated with the Froude number based on the following relation (Cui et al. 2015, Hübl et al. 2009):

$$\alpha = P_{\text{nmx}} / (\rho_{\text{p}} v^{2}) = a \cdot F r^{b} \tag{6}$$

where P_{max} is the maximum debris flow dynamic pressure, and a and b are constant coefficients.

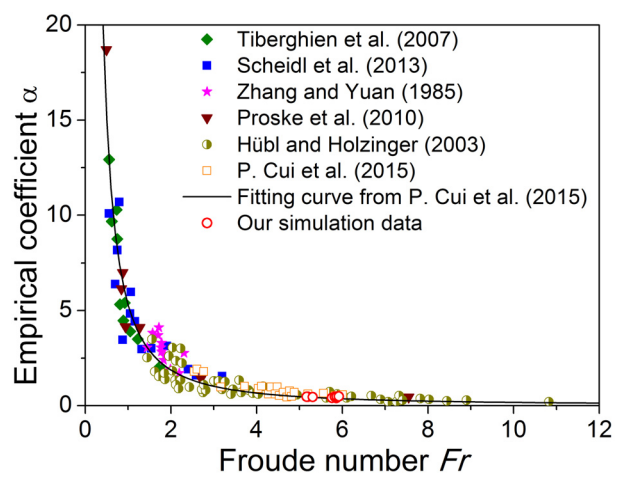


Figure 5. Correlation between the emperical coefficient α and Froude number Fr

As shown in Fig. 5, although the range of Froude number in our CFD-DEM simulations (open circles) is narrow with several overlapped points, our data collapse well onto the correlation curve between the empirical coefficient and the Froude number combining results from small-scale experiments to real-scale measurements. This serves as a validation of the present CFD-DEM approach in capturing the physical behaviour of debris flow and its impact on a rigid barrier.

4 CONCLUSION

We have examined the effect of fine exchange between fluid and solid phases in a debris flow on its impact behaviour on a rigid barrier using a coupled CFD-DEM approach. It is demonstrated that high-fraction fine exchange may cause the enhanced mobility and turbulence intensity of the mixture and induce vortex-like flow pattern when impacting occurs. The observations on the impact force evolution indicate a greater dominant role played by the fluid phase and a higher mobility of the debris mixture which lead to a larger maximum total impact force in cases with higher fine exchange. The relation between empirical coefficient α and Froude number Fr fits well with an existing empirical correlation corroborated by small-scale experiments and real-scale measurements.

5 ACKNOWLEDGEMENTS

The study was financially supported by the University Grants Council of Hong Kong by a Theme-based Research Scheme project T22-603/15N. The first author acknowledges the generous support of Hong Kong PhD Fellowship on her PhD study.

6 REFERENCES

- Arabnia, O. (2015). Particle size reduction in debris flows: laboratory experiments compared to field data from Inyo Cree, CA. Doctoral dissertation, San Francisco State University.
- Canelli, L., Ferrero, A. M., Migliazza, M., & Segalini, A. (2012). Debris flow risk mitigation by the means of rigid and flexible barriers experimental tests and impact analysis. *Natural Hazards and Earth System Sciences*, 12(5), 1693-1699.
- Cui, P., Zeng, C., & Lei, Y. (2015). Experimental analysis on the impact force of viscous debris flow. Earth Surface Processes and Landforms, 40(12), 1644-1655.
- Cundall, P. A., and Strack, O. D. (1979): A discrete numerical model for granular assemblies, *Geotechnique*, 29(1), 47-65. DOI: 10.1680/geot.1979.29.1.47.
- Hua, H. W., & Jermy, M. (2011). Effect of Turbulence Intensity on Vortex Formation Threshold in a Jet Engine Test Cell.
- Hübl, J., Suda, J., Proske, D., Kaitna, R., & Scheidl, C. (2009, September). Debris flow impact estimation. In Eleventh international symposium on water management and hydraulic Engineering (Vol. 1, pp. 137-148).
- Ilstad, T., Elverhøi, A., Issler, D., & Marr, J. G. (2004). Subaqueous debris flow behaviour and its dependence on the sand/clay ratio: a laboratory study using particle tracking. *Marine Geology*, 213(1), 415-438.
- Iverson, R. M. (1997). The physics of debris flows. *Reviews of geophysics*, 35(3), 245-296.
- Iverson, R. M. (2003). The debris-flow rheology myth. Debris-flow hazards mitigation: mechanics, prediction, and assessment, 1, 303-314
- Kafui, K. D., Thornton, C. and Adams, M. J. (2002): Discrete particle-continuum fluid modelling of gas-solid fluidised beds, *Chemical Engineering Science*, 57(13), 2395-2410. DOI: <u>10.1016/S0009-2509(02)00140-9</u>.
- Koch, D. L. and Hill, R. J. (2001): Inertial effects in suspension and porous-media flows, *Annual Review of Fluid Mechanics*, 33(1), 619-647. DOI: 10.1146/annurev.fluid.33.1.619.
- Leonardi, A. L. E. S. S. A. N. D. R. O., Wittel, F. K., Mendoza, M. I. L. L. E. R., & Herrmann, H. J. (2013). Multiphase debris flow simulations with the discrete element method coupled with a lattice-Boltzmann fluid. In *III International Conference on Particle-Based Methods-Fundamentals and Applications, Stuttgart* (pp. 276-87).
- O'Sullivan, C. (2011): Particulate discrete element modelling, *Taylor & Francis*.
- Scheidl, C., Chiari, M., Kaitna, R., Müllegger, M., Krawtschuk, A., Zimmermann, T., & Proske, D. (2013). Analysing debris-flow impact models, based on a small scale modelling approach. Surveys in Geophysics, 34(1), 121-140.
- Shan, T., & Zhao, J. (2014). A coupled CFD-DEM analysis of granular flow impacting on a water reservoir. Acta Mechanica, 225(8), 2449-2470.
- Wang, W., Chen, G., Han, Z., Zhou, S., Zhang, H., & Jing, P. (2016). 3D numerical simulation of debris-flow motion using SPH method incorporating non-Newtonian fluid behavior. *Natural Hazards*, 81(3), 1981-1998.
- Yang, H., Wei, F., Hu, K., Chernomorets, S., Hong, Y., Li, X., & Xie, T. (2011). Measuring the internal velocity of debris flows using impact pressure detecting in the flume experiment. *Journal of Mountain Science*, 8(2), 109-116.
- Zhao, J., & Shan, T. (2013a). Numerical modeling of fluid-particle interaction in granular media. *Theoretical and Applied Mechanics Letters*, 3(2), 021007.
- Zhao, J., & Shan, T. (2013b). Coupled CFD–DEM simulation of fluid– particle interaction in geomechanics. *Powder technology*, 239, 248-258
- Zhou, Z. Y., Kuang, S. B., Chu, K. W., & Yu, A. B. (2010). Discrete particle simulation of particle–fluid flow: model formulations and their applicability. *Journal of Fluid Mechanics*, 661, 482-510.